Angewandte Chemie
Eine Zeitschrift der Gesellschaft Deutscher Chemiker

Supporting Information

Transformable Peptide Nanocarriers for Expeditious Drug Release and Effective Cancer Therapy via Cancer-Associated Fibroblast Activation

*Tianjiao Ji, Ying Zhao, Yanping Ding, Jing Wang, Ruifang Zhao, Jiayan Lang, Hao Qin, Xiaoman Liu, Jian Shi, Ning Tao, Zhihai Qin, Guangjun Nie, and Yuliang Zhao**

anie_201506262_sm_miscellaneous_information.pdf

SUPPORTING INFORMATION

Contents

Experimental Section

Enzyme-responsiveness of CAP and UAP. Recombinant human fibroblast activation protein α-FAP (rhFAP; R&D system, USA) was diluted to 0.2 mg/mL in assay buffer (50 mM Tris, 1 M NaCl, 1mg/mL BSA, pH 7.5). After 50 μL of 0.2 μg/mL of rhFAP was loaded into a plate, the reaction was started by adding 50 μL of 100 μM CAP (dissolved in assay buffer) or UAP, respectively. After 3 h, the reaction product was analyzed by matrix-assisted laser desorption/ionization time of flight mass spectrometry (MALDI-TOF MS) (Bruker, Germany). The MS detection range was 500-2000 Da. For recombinant human DPPIV/CD26 (rhDPPIV; R&D system, USA) reactions, the assay buffer used consisted of 25 mM Tris, pH 8.0, and the CAP or UAP concentration was 20 μM.

Determination of critical micelle concentration. The amphiphilic peptides (CAP and UAP) were synthesized by GL Biochem Ltd. (Shanghai, China) via Fmoc solid phase peptide synthesis. A series of concentrations of CAP or UAP (0 to 200 μM) were incubated with a pyrene solution (24 μg/L) for 1 h. A fluorescence spectrophotometer (HITACHI F-4600, Japan) was used to measure the fluorescence intensity of each mixture (excitation at 330 nm). The ratios between the intensities at 384 nm and 373 nm were used to calculate the critical micelle concentration (CMC) of the peptide in PBS.

Self-assembly of CAP and UAP. 0.05 mg CAP or UAP was dissoved in 5 μL dimethyl sulfoxide (DMSO) (Sigma Aldrich, USA), and then added into 1 mL distilled water to be ultrasonicated (KQ2200E, China) at 100 W for 1 min. The resulted nanostructures was characterized by transmission electron microscopy (TEM, Tecnai G2 F20 U-TWIN) using a negative staining method with phosphotungstic acid at different times of incubation. The thickness of resulted nanofibers was analyzed by atomic force microscopy (AFM; Dimension 3100, Bruker, USA). Briefly, the aqueous solutions of self-assembled CAP or UAP (0.05 mg/mL) were drop-casted on a freshly cleaved mica surface. After 10 min adsorption, excess solution was removed from the mica surface before AFM analysis. Tapping-mode AFM experiments were performed under ambient conditions. Commercial silicon tips with a nominal spring constant of 2.0 N/m and resonant frequency of 442.5 kHz were used in all the AFM imaging.

Drug-induced reassembly of CAP nanostructures. 0.03 mg hydrophobic drug (Dox, Iri or Tax) was dissolved in 5μL DMSO and mixed with solution of self-assembled peptide by ultrasonication (100 W), then incubated for 5 min at room temperature prior to TEM analysis. Mouse serum was added to the reassembled solution (30% serum, final concentration) and incubated for 48 h to evaluate the

stability of nanoparticles. For TEM analysis of nanostructures, a negative staining (phosphotungstic acid, 10 min) was used.

Preparation and characterization of drug-loaded nanoparticles. CAP or UAP (1.0 mg) and a chemotherapeutic drug (Table S1) were dissolved in 10 μL DMSO. This solution was added to 2 mL PBS and ultrasonicated (100 W) for indicated time (Dox-loading, 5 min; Iri-loading, 12 min; Tax-loading, 20 min). The solution was then incubated at room temperature for 1 h. The aqueous phase was collected after centrifugation at 6,000 g for 5 min at room temperature.

The morphology, particle size distribution, and zeta potential of NPs were characterized by TEM using a negative staining method with phosphotungstic acid and dynamic light scattering (DLS, Zetasizer Nano ZS90, Malvern, UK), respectively. For evaluating Dox or Iri encapsulation efficiency, lyophilized drug-loaded nanoparticles were dissolved in DMSO and measured by UV-Vis spectrophotometer (LAMBDA650, PerkinElmer, USA) after making a standard curve with free drug. For Tax encapsulation efficiency calculation, the original mass of drug was measured, and the mass of sediment after encapsulation was considered to be that of the unloaded Tax. The encapsulation efficiency (EE) was calculated according to the following formula:

$$EE\ (\%) = (\text{mass of drug encapsulated in nanoparticles/mass of drug added}) \times 100\%$$

The *in vitro* drug release kinetics of CAP-Dox and UAP-Dox was measured *via* dialysis. Briefly, 1 mL CAP-Dox or UAP-Dox solution was injected into dialysis cartridge with a molecular weight cut-off value of 2 kDa. The cartridge was dialyzed against 10 mL PBS (10% FBS) and shaken at 37 ℃ at 100 rpm with activated charcoal to create an ideal sink condition. The concentration of Dox remaining in the dialysis cartridge at different time points was measured by UV-Vis spectrophotometry.

Cell culture and animals. PF179T-CAF cells (prostate CAFs, hTERT immortalized, constructed by Department of Urology, University of Innsbruck, Austria) were generously provided by Prof. Ju Zhang. PC-3 (prostate cancer cell), Mia-Paca-2 (pancreatic cancer cell), MCF-7 (breast cancer cell) and HUVEC (human umbilical vein endothelial cell) lines were purchased from the National Platform of Experimental Cell Resources for Sci-Tech (China). All cell lines were passaged in the laboratory for less than 3 months after resuscitation and maintained in a 37℃ / 5% CO_2 humidified chamber. HUVECs and MCF-7 cells were maintained in Dulbecco's modified Eagle's medium (DMEM) supplemented with 10% FBS (WISENT, Canada); Mia-paca-2 were grown in RPMI-1640 media with

10% FBS; and CAFs and PC-3 were maintained in Ham's F12K (WISENT, Canada) with 10% FBS, 1% GlutaMax (Introvigen, USA), 1% Na-pyruvate (Invitrogen, USA), 1% NEAA (Invitrogen, USA).

BALB/c nude mice were purchased from Vital River Laboratory Animal Technology Co. Ltd. All animal protocols were approved by the Institutional Animal Care and Use Committee. In the prostate tumor model, CAFs and PC-3 cells (2.5×10^6 each) were suspended in a 100 μL PBS and Matrigel mixture (1:1, v/v; BD, USA), and subcutaneously co-inoculated at the back of each nude mouse (male, 6 weeks age, 16-18 g body weight); for pancreatic tumor model, 5×10^6 Mia-paca-2 cells were used and subcutaneously inoculated at the underarm of fore limb of each nude mouse (male, 6 weeks age, 16-18 g body weight); for breast tumor models, 5×10^6 MCF-7 cells were inoculated at mammary fat pad of each nude mouse (female, 6 weeks age, 15-17 g body weight).

Confocal microscopy tracking of Dox in live cells. CAFs, PC-3 and HUVEC cells were seeded in confocal dishes (Nunc, USA). When the cells were 70% confluent, they were incubated with CAP-Dox or UAP-Dox (1 μM Dox) for 4 or 24 h at 37℃. Cells were then washed 3 times with PBS to be observed by confocal microscopy (LSM710, Carl Zeiss, Germany). In the cell co-culture system, CAFs at 40% confluence were stained with CellTrace™ Calcein Violet, AM (Invitrogen, USA) for 40 min. Then, Calcein AM (Invitrogen, USA) labeled PC-3 cells were added to the chamber. After 24 h, CAP-Dox or UAP-Dox (1 μM Dox) was added for further incubation of 4 h at 37℃. The cells were then washed 3 times with PBS and observed using confocal microscopy.

Cytotoxicity Studies. For the in vitro cell viability assay, CAF, PC-3 and HUVEC cells were seeded in 96-well plates, and cultured with CAP-Dox and UAP-Dox for 24 hours when cells were 70% confluent. The drug concentration varied from 0-5 μM. The amount of viable cells was evaluated via a CCK-8 assay (Dojindo, Japan). After 2 hours of treatment, the absorbance at 545 nm, was detected with a microplate reader. Reference wavelength was set at 660 nm. Untreated cells served as control. Results are shown as the average cell viability [(OD treat OD blank)/(OD control OD blank) ×100%] of quintuplicate wells.

Construction of fluorescent CAP nanoprobe (CAP-RB) and assessment of *in vivo* distribution. For the CAP-RB assembly, 0.5 mg CAP, 0.1 mg Tetramethylrhodamine isothiocyanate (TRITC) (Sigma Aldrich, USA) and 0.1 mg Black Hole Quencher (BHQ-1) (Sigma Aldrich, USA) were dissolved in 10 μL DMSO. The solution was added to 1 mL PBS, ultrasonicated (100 W, 5 min) and

incubated at room temperature (25 ℃) for 1 h. Next, the aqueous phase was collected after centrifugation at 6,000 g for 5 min at room temperature.

Nude mice bearing the three types of tumors were intravenously injected with CAP-RB (100 μL). The mice were then scanned with a Maestro *in vivo* imaging system (CRI, Woburn, MA, USA). The scanned excitation wavelength was 520-560 nm and the emission wavelength was 590 nm.

To estimate the blood clearance rate of CAP nanocarrier *in vivo*, TRITC and CAP-R were intravenously injected into normal BALB/c mice, respectively. At different time points, blood was collected and measured for fluorescence signal by Maestro *in-vivo* imaging system.

For biodistribution measurement, nude mice bearing subcutaneous prostate (CAFs + PC-3 cells) tumors were intravenously injected with CAP-R (100 μL, with 0.5 mg/mL of CAP peptide). Mice were scanned with Maestro *in vivo* imaging system. At 5 h after injection, organs and tumors were excised for *ex vivo* imaging.

Stability of CAP nanocarrier in blood. Human serum was obtained from Beijing Red Cross Blood Center (approved by Institutional Ethics Committee). CAP-R and TRITC were incubated with mouse blood or serum for 4 h. Then serum component was isolated from the blood incubation system. The fluorescence intensity was examined at the excitation wavelength of 550 nm and emission wavelength of 580 nm. Meanwhile, CAP-RB was incubated with human serum in the presence or absence of FAP-α for different time intervals. The fluorescence intensity at each time point was examined. Furthermore, the dispersity of CAP-Dox and hydrophobic Dox in human serum was also investigated to reflect the stability of CAP-Dox.

Therapeutic studies. For the subcutaneous xenograft mouse model of PC-3/CAF prostate cancer, treatment was initiated on day 11 after inoculation, when tumor volume reached 100 mm^3. Mice were administered (iv) with PBS, CAP, Dox, CAP-Dox or UAP-Dox (n = 8). A dose of 5 mg/kg Dox was given every 3 days for a total of 4 injections. Tumor sizes were measured by a digital caliper, and tumor volume was calculated by the formula $(L \times W^2)/2$, where L is the longest and W is the shortest in tumor diameters (mm). Relative tumor volume (RTV) equals the tumor volume at a given time point divided by the tumor volume before treatment started. For humane reasons, and for further research, animals were sacrificed when the implanted tumor volume reached 800 mm^3 (day 15). The hearts, livers and kidneys were subject to post-mortem histopathology analysis; the tumors to morphology and immunohistochemistry (IHC) analysis. For IHC, mouse anti-human α-smooth muscle actin (α-SMA)

monoclonal antibody (Abcam, UK) was used at 8 μg/mL for 1 h at 37 ℃. CAFs were detected by an anti-mouse HRP-DAB cell and tissue staining kit (R&D system, USA), and hematoxylin (Solarbio, China) was used to stain the tissue.

For evaluation of apoptosis in tumor cells, tumor tissue sections were stained by terminal deoxynucleotidyl transferased dUTP nick end labeling (TUNEL; KeyGEN BioTECH, Nanjing, China) according to the manufacturer's protocol. The nuclei were counterstained with DAPI. Sections were examined by confocal microscopy. A total of 100 nuclei over two separate slides were examined to obtain quantitative results. To evaluate necrosis, we stained sections with H&E and analyzed them using a light microscopy (AMG EVOS xl core, Life Technologies).

For the pancreatic and breast tumor models, treatment was initiated on day 23, when tumor volume reached 100 mm^3. Iri (25 mg/kg) or Tax (5 mg/kg), either free or encapsulated by CAP or UAP, was given every 2 days for a total of 9 (Iri) or 5 (Tax) doses. For IHC analysis, mouse anti-human α-smooth muscle actin (α-SMA) monoclonal antibody (Abcam, UK) or mouse anti-human FAP-α monoclonal antibody (Abcam, UK) was used at 8 μg/mL for 1 h at 37 ℃. CAFs were detected as described above.

Evaluation of Dox penetration in tumors. Dox, CAP-Dox and UAP-Dox (Dox dose: 5 mg/kg) were intravenously injected into PC-3/CAF prostate tumor-bearing nude mice. After 24 hours, excised tumours were frozen in optimum cutting temperature (OCT) medium (Sakura Finetek, USA) at -80 ℃. The corresponding slices (6 μm) were prepared, air dried for 10 minutes, and fixed with 4% paraformaldehyde (Solarbio, China) for 10 min. The nuclei were counterstained with 4', 6-dia-midino-2-phenylindole (DAPI) (Invitrogen, USA), and the tumor blood vessels were stained with CD31 (Abcam, UK). Slices were observed by confocal microscopy.

Western blot. CAF, PC-3, MCF-7, and Mia-paca-2 cells were lysed with RIPA buffer (Solarbio, China) containing 1 mM phenylmethanesulfonyl fluoride (PMSF) (Solarbio, China). Tumors were pulverized in liquid nitrogen before lysis. Protein samples (40-80 μg) were electrophoresed on 10% sodium dodecyl sulfate–polyacrylamide gels. The proteins were then transferred onto a polyvinylidene fluoride (PVDF) membrane. Loading and transfer were then confirmed by Ponceau red staining. After preincubation in blocking solution at room temperature for 1 hour, the PVDF membrane was incubated with mouse anti-human FAP-α monoclonal antibody (1:1,000) (Abcam, UK) for 2.5 hours at room temperature. After being washed 3 times for 5 min with Tris-buffered saline (TBS) containing 0.5% Tween-20 (Solarbio, China), the membrane was incubated with a secondary antibody linked to

horseradish peroxidase (goat anti-mouse IgG, 1:10,000) (Santa cruz, USA) for 50 min at room temperature. Immunoreactive proteins were visualized using SuperSignal West Pico Chemiluminescent Substrate (Thermo Scientific, Rockford, USA).

Statistical analysis. Statistical analysis was conducted by the Student t test for comparison of 2 groups, and one-way ANOVA for multiple groups, followed by Newman–Keuls test if overall $P < 0.05$. A p value of less than 0.05 was considered significant (*), while a p value of less than 0.01 was considered very significant (**).

Supplementary Tables and Figures

Table S1. Characterization of drug-loaded NPs

Groups	Particles size (nm)	Zeta potential (mV)	Polydispersity
CAP-Dox	68.3±5.7	-15.7±0.3	0.34
UAP-Dox	66.8±4.6	-21.6±0.4	0.33
CAP-Iri	75.8±5.2	-16.2±0.5	0.35
UAP-Iri	72.6±5.1	-22.7±0.3	0.37
CAP-Tax	58.5±4.2	-15.8±0.6	0.36
UAP-Tax	59.6±4.7	-20.8±0.4	0.35

All results were determined by DLS. Nanoparticles were prepared by dissolving in PBS at a concentration of 0.5 mg/mL. Results are mean ± S.D. (n=3).

Table S2. Encapsulation efficiencies of CAP-Dox, UAP-Dox, CAP-Iri, UAP-Iri, CAP-Tax and UAP-Tax with different mass of drug added (the mass of CAP or UAP used was 0.5 mg)

	Dox added (μg)	30	60	120	180	240	300
CAP-Dox	**Dox encapsulated (μg)**	29.5	52.1	92.2	131	145	145
	Encapsulation efficiency (%)	98.3	86.8	76.8	72.9	60.5	48.4
UAP-Dox	**Dox encapsulated (μg)**	27.2	49.7	91.5	142	144	143
	Encapsulation efficiency (%)	90.7	82.8	76.3	78.6	59.8	47.6
	Iri added (μg)	50	100	200	300	400	500
CAP-Iri	**Iri encapsulated (μg)**	49.4	93.6	159	228	259	243
	Encapsulation efficiency (%)	98.7	93.6	79.3	76.1	64.7	48.5
UAP-Iri	**Iri encapsulated (μg)**	49.4	92.8	160	228	263	250
	Encapsulation efficiency (%)	98.8	92.8	79.9	75.9	65.7	50.0
	Tax added (μg)	100	200	300	400	500	600
CAP-Tax	**Tax encapsulated (μg)**	95	122	146	159	167	149
	Encapsulation efficiency (%)	95.0	61.0	48.7	39.8	33.4	24.8
UAP-Tax	**Tax encapsulated (μg)**	93	126	132	153	171	152
	Encapsulation efficiency (%)	93.0	63.0	44.0	38.3	34.2	25.3

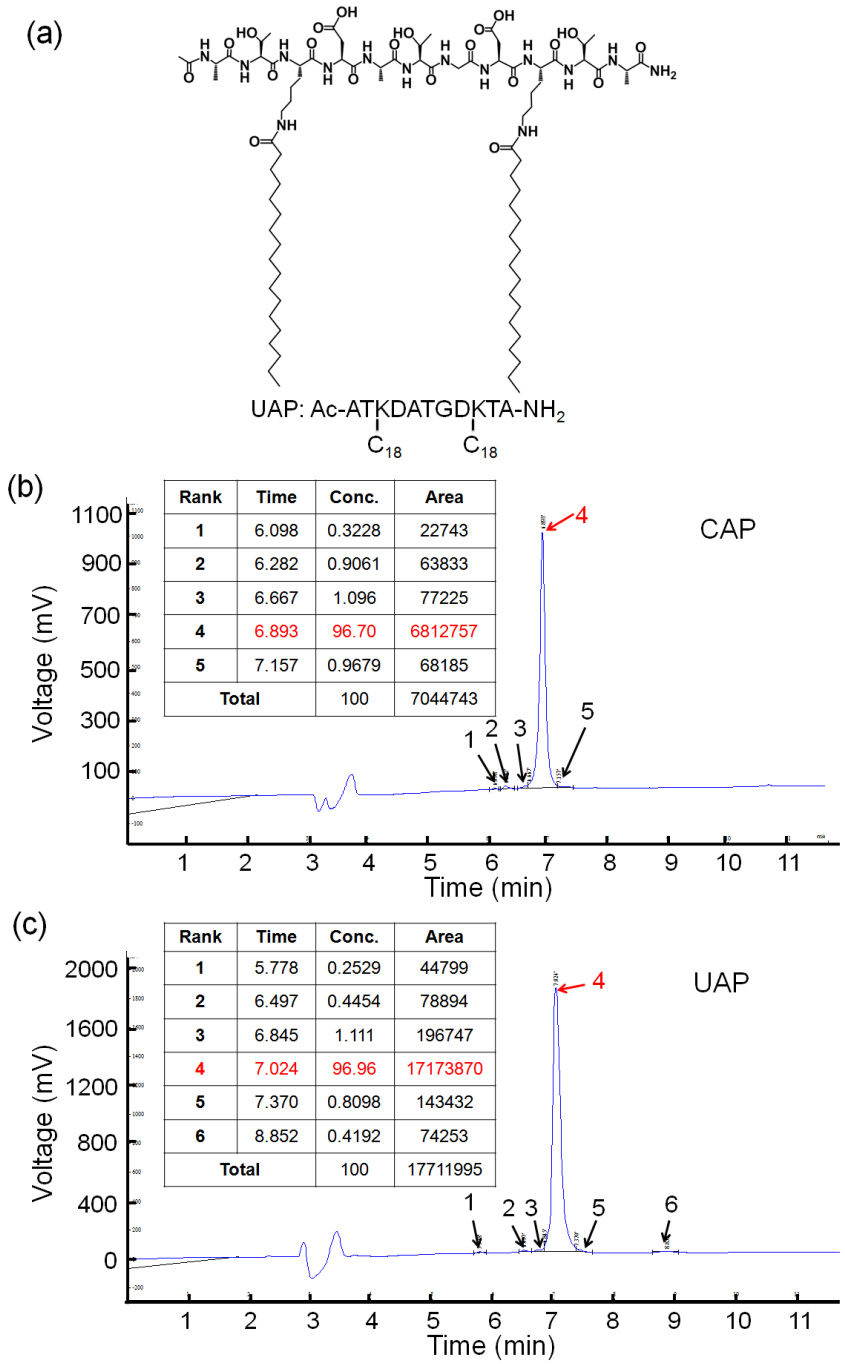

Figure S1. a) The structure of UAP. UAP has a similar structure to CAP but is lack of the FAP-α responsive sequence. b, c) HPLC analysis of CAP and UAP. Both peptides have a purity of over 95%.

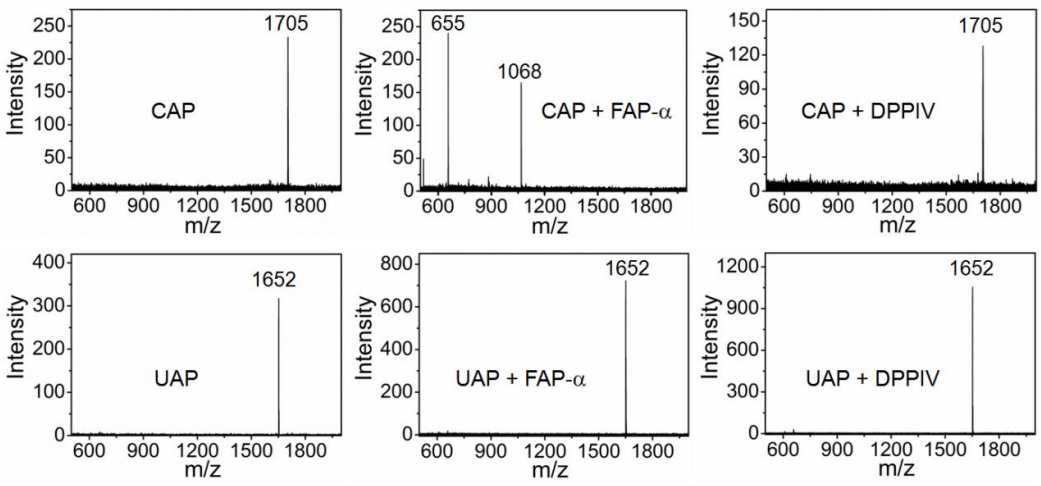

Figure S2. The enzyme responsiveness of CAP and UAP. The cleavage (or lack thereof) of two amphiphilic peptides (concentration: 50 μM) by FAP-α or DPPIV as demonstrated by MALDI-TOF.

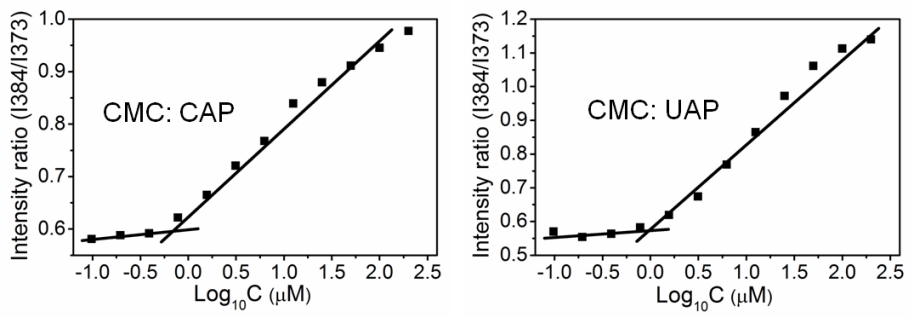

Figure S3. The CMCs of CAP and UAP. The CMC of CAP is 0.66 μM and the CMC of UAP is 0.89 μM.

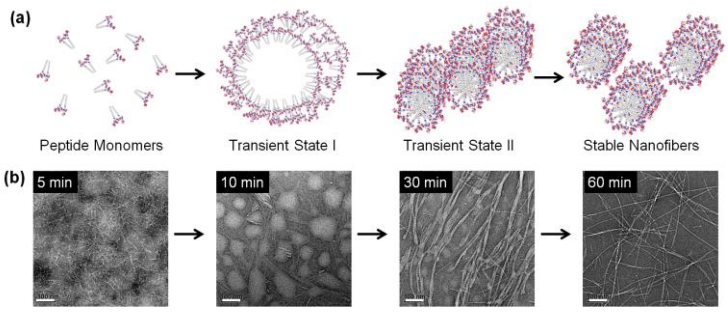

Figure S4. a) The schematic mechanism of peptide self-assembly. b) TEM examination of the self-assembly of UAP. The assembled product changed from irregularly shaped aggregates to nanofibers as time elapsed. The scale bar is 100 nm.

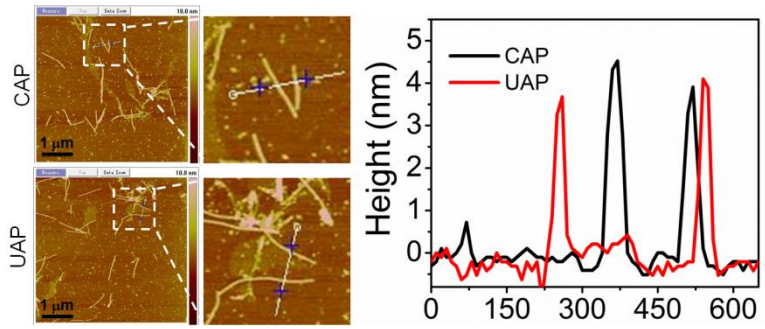

Figure S5. The thickness of CAP and UAP self-assembled nanofibers as measured by AFM. The thickness of two APs self-assembled nanofibers is about 4 nm. The scale bar in AFM images is 1 μm.

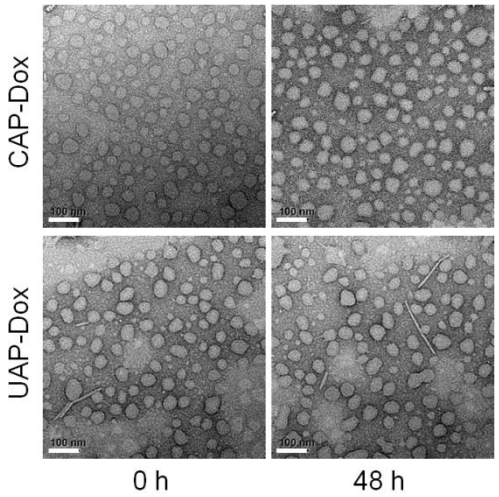

Figure S6. The stability of hydrophobic Dox-induced reassembly of nanoparticles in a serum-containing solution. Both CAP-Dox and UAP-Dox exhibited no change in morphology after incubation with serum-containing solution for 48 h. The scale bars are 100 nm.

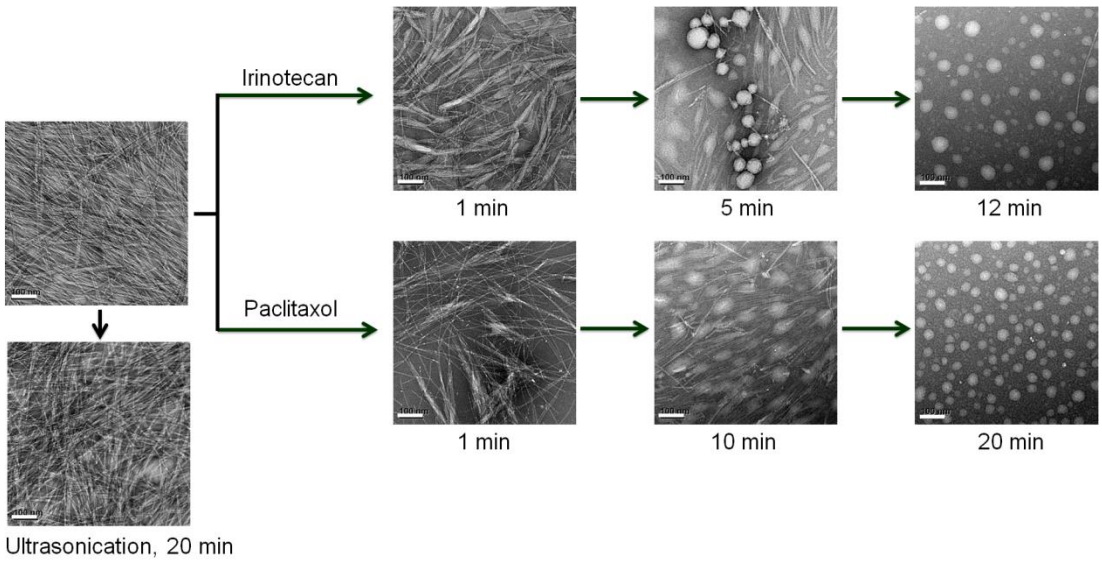

Figure S7. TEM examination of the morphology changes during the encapsulation of the other two hydrophobic drugs (Iri and Tax). Scale bar is 100 nm.

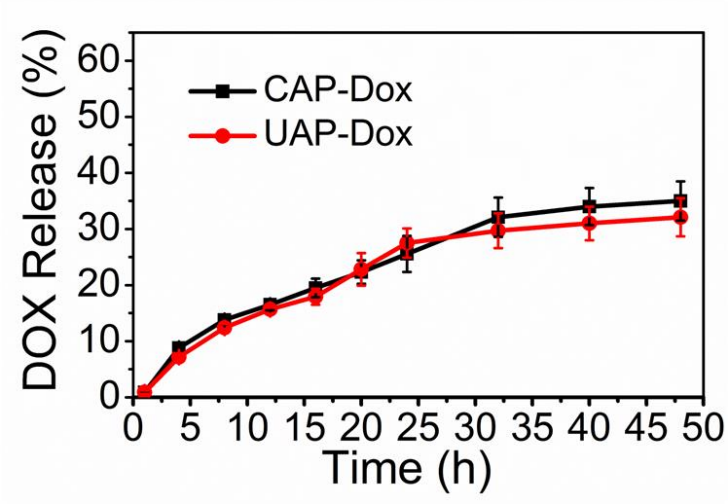

Figure S8. The drug release profiles of CAP-Dox and UAP-Dox in the absence of FAP-α.

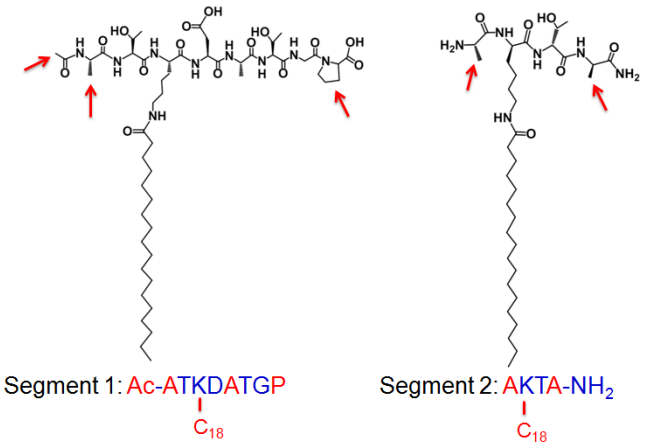

Figure S9. The two segments of CAP after cleavage by FAP-α. The red arrows indicate the hydrophobic amino acid residues.

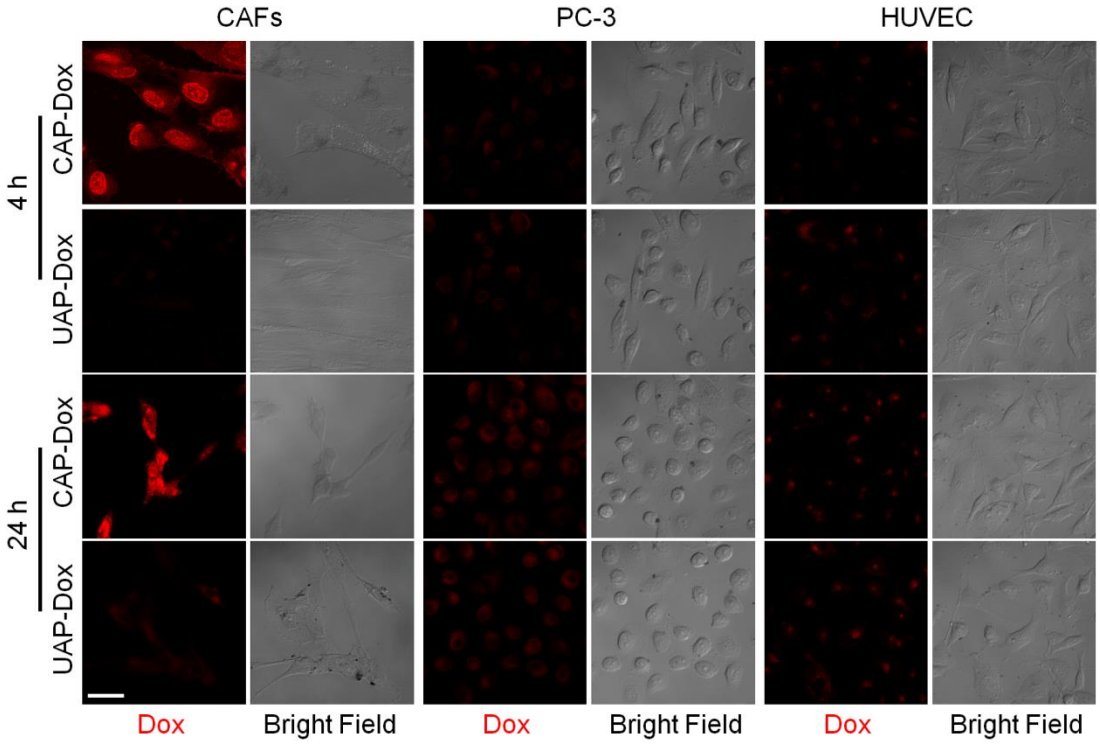

Figure S10. Evaluation of the cellular uptake of Dox after incubating CAFs, PC-3 and HUVECs with either CAP-Dox or UAP-Dox for 4 or 24 h. Dox fluorescence was detected by confocal microscopy. Scale bar is 50 μm. Only CAFs in the CAP-Dox group exhibited efficient Dox uptake, while the other cell types did not exhibit large amounts of Dox uptake.

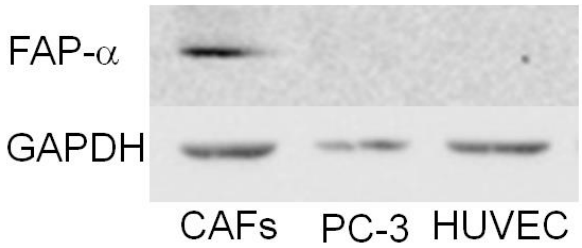

Figure S11. Western blot analysis of FAP-α expression in three cell lines. CAFs were FAP-α positive, and PC-3 and HUVEC were FAP-α negative.

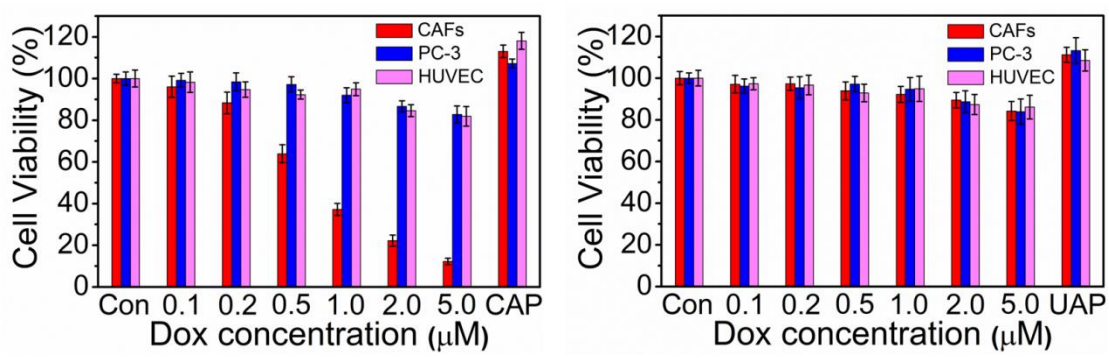

Figure S12. Cytotoxicity of CAP-Dox (left panel) and UAP-Dox (right panel) in CAFs, PC-3 and HUVECs measured by CCK-8 assay.

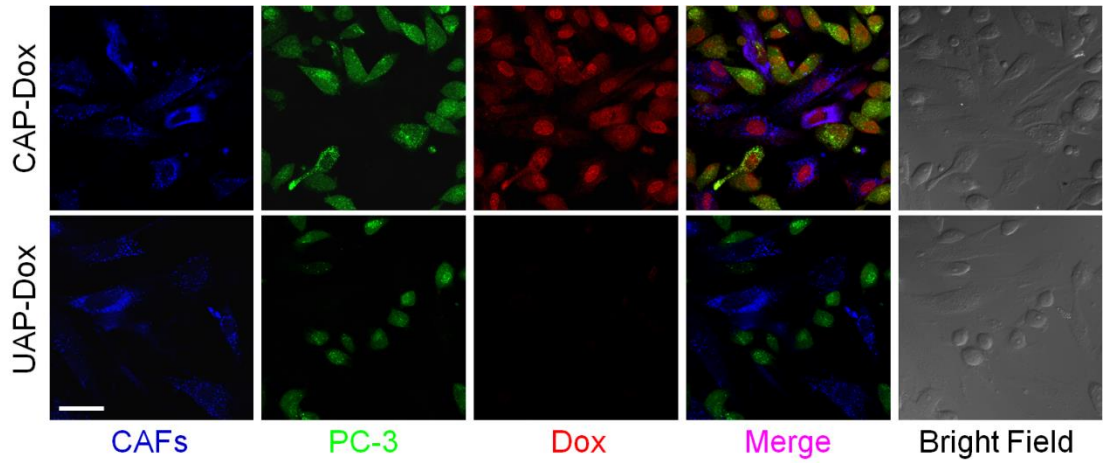

Figure S13. Cellular uptake of Dox in a PC-3 and CAF co-culture system. CAFs were labeled by CellTrace™ Calcein Violet, AM (blue) and PC-3 cells were labeled by Calcein AM (green). Red: Dox. Scale bar is 50 μm.

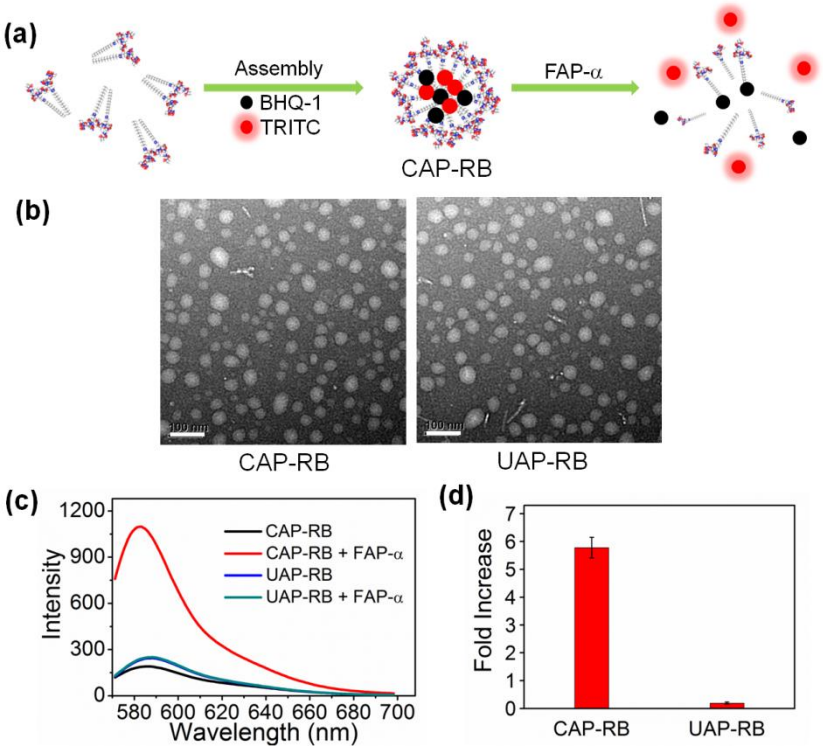

Figure S14. a) Schematic illustration of the construction of fluorescent peptide nanoprobes. A hydrophobic dye (tetramethyl rhodamine isothiocyanate mixed isomers**,** TRITC) and its quencher (black hole quencher-1, BHQ-1) were loaded at a ratio of 1:1 into CAP or UAP (CAP-RB or UAP-RB). By fluorescence resonance energy transfer (FRET), the dye encapsulated in CAP-RB or UAP-RB remained in the quenched state. The FAP-α can only cleave CAP-RB to release the quencher and enhanced the fluorescence. b) The TEM morphologies of CAP-RB and UAP-RB. The scale bar is 100 nm. c, d) The fluorescence intensity of CAP-RB and UAP-RB with or without FAP-α incubation. CAP-RB exhibited a 6-fold increase in fluorescence after activation by FAP-α.

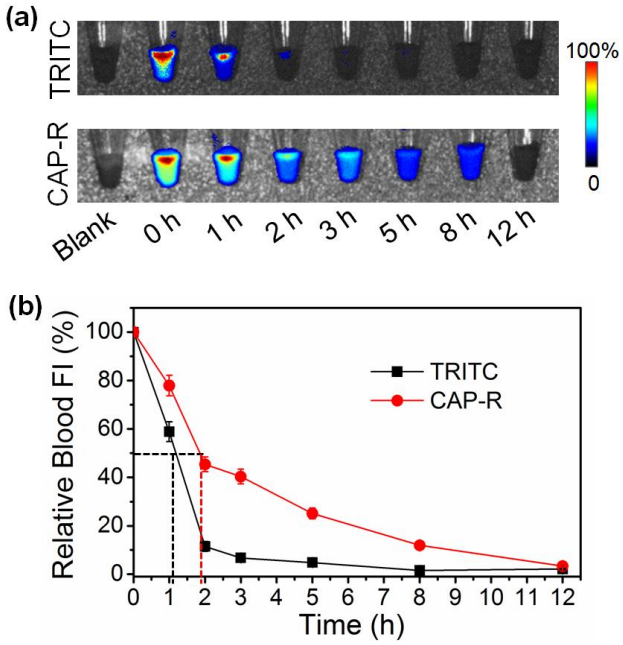

Figure S15. The blood clearance rate of CAP-R *in vivo*. BALB/c mice were intravenously injected with TRITC or CAP-R. At different time points, blood was collected and detected for fluorescence signal by *in vivo* imaging system (a). Relative fluorescence intensity (FI) was calculated and quantified (b). The half-life of CAP-R nanoparticles in circulation was about 2 h, while the free fluorescence dye, TRITC, was about 1 h.

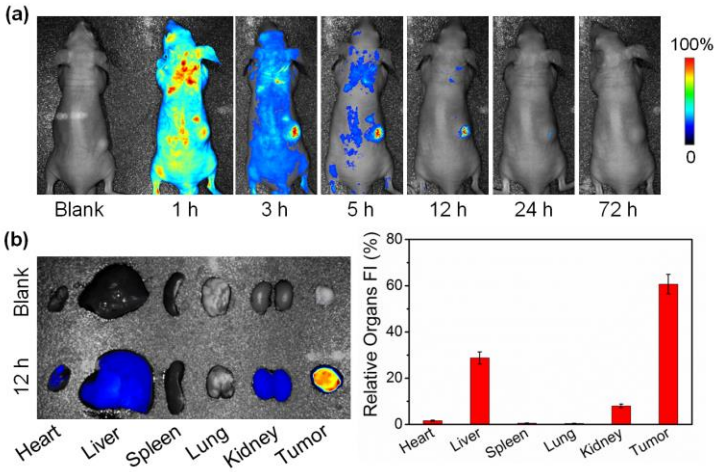

Figure S16. The evaluation of the biodistribution of CAP-R. a) The CAP-R distribution at different time points in CAFs and PC-3 co-implanted prostate tumor bearing mice. b) The *ex vivo* imaging of major organs 12 h after injection of CAP-R (left). Relative fluorescence intensity (FI) in each organ of lower panel was calculated and quantified (right).

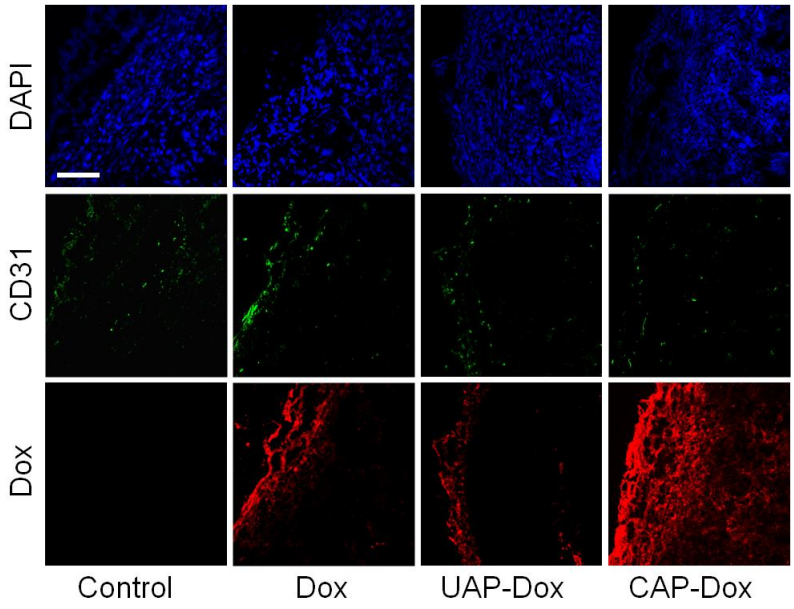

Figure S17. The split channels of Figure 4b.

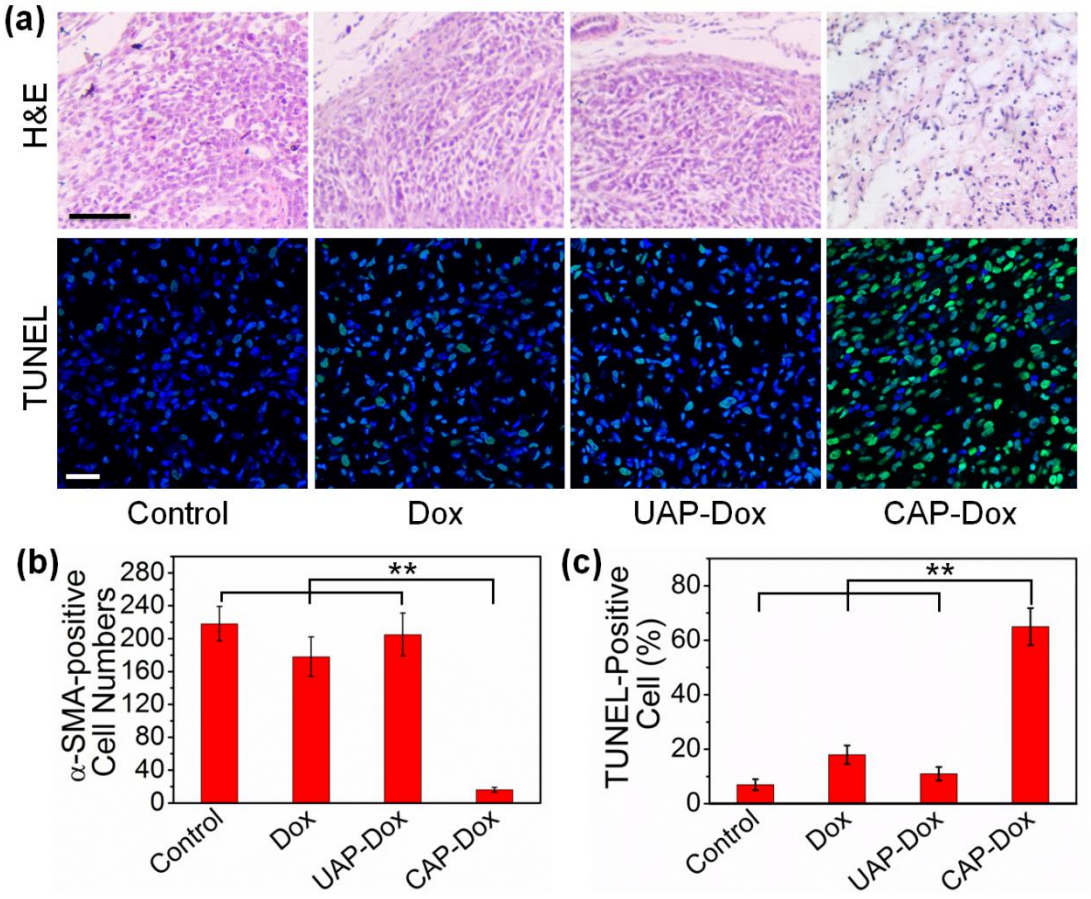

Figure S18. a) Staining of tumor slices treated with the indicated formulations. H&E staining, top row; TUNEL immunofluorescence staining, bottom row, blue: DAPI, green: apoptosis signal. Scale bars, 50 μm. b) Numbers of α-SMA positive cells in tumors treated by the indicated drug formulations. Cells from tumor slices of five randomly chosen fields were counted for α-SMA staining under a light microscope. Data are presented as mean ± S.D. **p<0.01 vs. control, Dox, and UAP-Dox groups. c) Percentage of TUNEL positive apoptotic cells in tumors treated by the indicated drug formulations. The apoptotic rates were evaluated as the percentage of apoptotic cells in each field. Five random selected fields were examined under a confocal microscope. Data are presented as mean ± S.D. **p<0.01 vs. control, Dox and UAP-Dox groups.

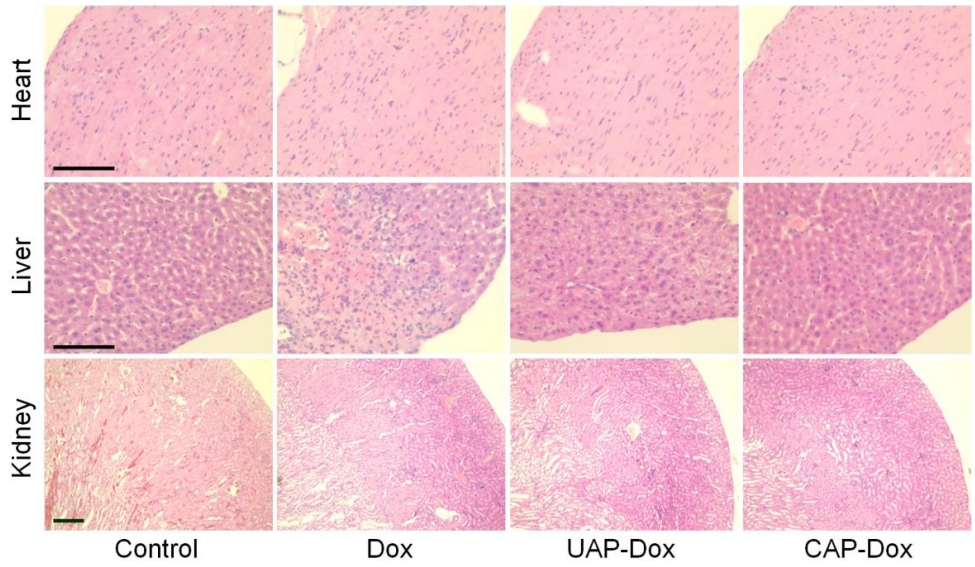

Figure S19. H&E staining of tissue slices of hearts, livers and kidneys from normal mice treated with free Dox, UAP-Dox or CAP-Dox (5 mg/kg Dox). Scale bars in heart and liver slices are 50μm, in kidney slices is 100 μm.

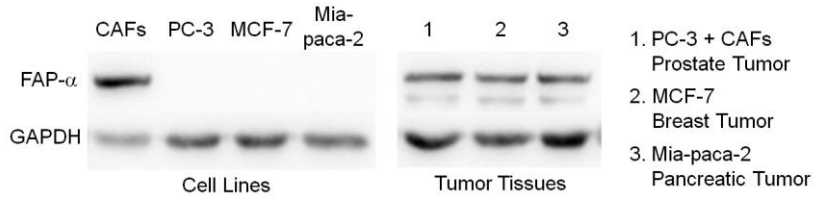

Figure S20. Western blot analysis of FAP-α expression in three different tumor cell lines (PC-3, MCF-7, Mia-paca-2) and their correspondent tumor xenografts.

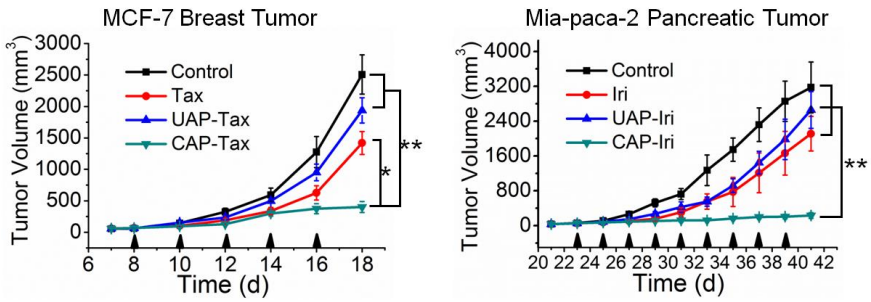

Figure S21. *In vivo* antitumor efficacy of CAP-encapsulated chemotherapeutic drugs in breast cancer and pancreatic cancer xenografts (n = 6). Tax-dose, 5 mg/kg; Iri-dose, 25 mg/kg. (*p<0.05; **p<0.01, CAP nanocarriers vs. drug-containing groups).

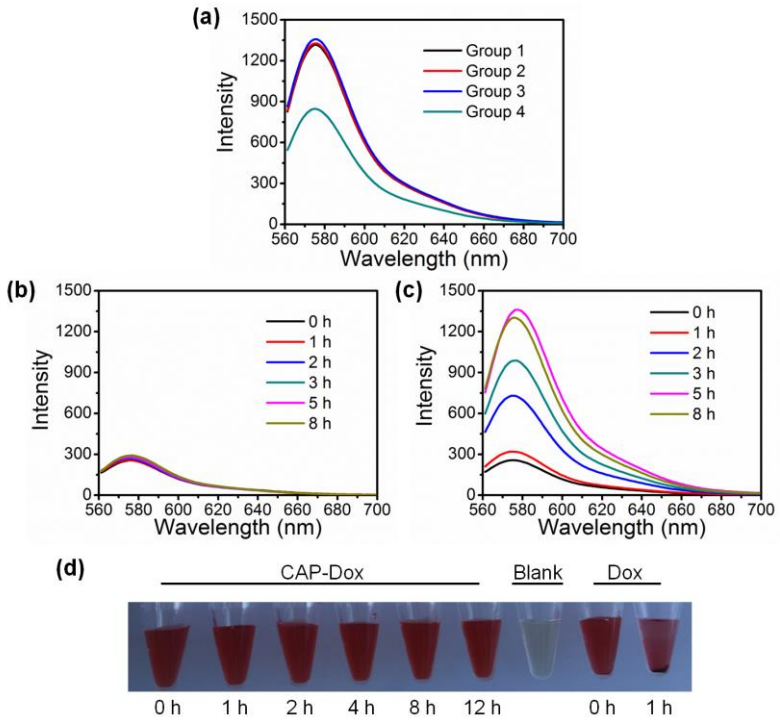

Figure S22. Stability of CAP nanocarrier in blood. a) The fluorescence intensity of CAP-R and TRITC after incubation with mouse blood and serum. The CAP-R was incubated with blood (Group 1) or serum (Group 2) for 4 h. TRITC incubated with blood (Group 3) or serum (Group 4) served as controls. After isolation of the serum component of Group 1 and Group 3, the fluorescence intensity of the serum in four groups was measured. Compared with Group 4, the fluorescence intensity was dramatically decreased in Group 3, indicating that some free TRITC may enter blood cells. In contrast, the fluorescence intensity of Group 1 and Group 2 was almost identical, indicating that CAP-R cannot be taken up by blood cells and no significant fluorescent dye was released into serum. b) The fluorescence intensity of CAP-RB in human serum for different time intervals. c) The fluorescence intensity of CAP-RB in human serum containg FAP-α for different time intervals. d) The dispersibility and stability of CAP-Dox and Dox in human serum. The CAP-Dox and free hydrophobic Dox were incubated with human serum. After incubation for 12 h, CAP-Dox uniformly dispersed in the serum. However, free Dox precipitated in serum only after incubation for 1 h.